

A New Anti-Windup PI Controller for Direct Torque Control System

MIAO Jing-Li*, LI Qi-meng
Hebei University of Engineering, China
*Corresponding author, e-mail: 871666238@qq.com

Abstract

Speed controller in induction motor direct torque control (DTC) system usually adopts the traditional PI controller. But the traditional PI controller has characteristic of nonlinear saturation, what will make the control performance of actual system become worse. In order to improve system control performance, this paper adopts a new type Anti-Windup PI controller, This method separately control the integral state by feed backing the output of the integrator to the input port of the integrator according to whether the controller output is saturated or not, which can make the system leaving saturation as soon as possible. As a result, the overshoot and settling time of the system are reduced. Simulation and experimental results show that this method can significantly suppress the integral windup phenomenon as well as reduce the overshoot and shorten the settling time. The new Anti-Windup PI controller has a better performance than the traditional PI controller.

Key words: induction motor; direct torque control; PI controller; Anti-Windup; simulation

Copyright © 2014 Institute of Advanced Engineering and Science. All rights reserved.

1. Introduction

Direct torque control (DTC) technology is a high-performance AC speed regulating technique. It appears later than the vector control technology. But compared with vector control technology, DTC technology will not be restricted by current regulator bandwidth. So the torque dynamic response is faster and not sensitive to the change of the parameters of motor [1-5]. But a typical speed controller of DTC system usually uses PI controller. While the traditional PI controller does not consider the upper limit of actual torque. When the mutation in the speed is happened, PI controller will output a big torque. But actually the motor can't output such a big torque. It will make the performance of the system become worse. We call this phenomenon Windup [6-10].

To solve this problem, this paper adopts a new type Anti-Windup PI controller. The new controller can quickly exit the saturated zone, So as to realize the reducing of overshoot and faster response speed [11-14].

2. New Anti-Windup PI Controller

In the induction motor, the relationship between speed and torque is:

$$\frac{d\omega}{dt} = \frac{(T_E^* - T_L)}{J} - \frac{\omega}{J/B} \quad (1)$$

Using s-function can be expressed as:

$$\omega = \frac{(T_E^* - T_L)}{Js + B} \quad (2)$$

In the equation, ω is angular velocity of the mechanical rotor, J is the moment of inertia of the motor, B is the Viscous friction coefficient, T_E^* is the given torque of the motor, T_L is the

load torque, J/B is called the mechanical time constant. Let $k_m=J/B$, that is to say k_m is mechanical time constant.

Traditional PI controller is affected by the Windup phenomenon, its equivalent on the output side joined a limiting function $T_E^*(u)$. Equation (3) is the expression. Figure 1 is the function of the corresponding curve. Figure 2 is the PI controller structure with a saturation limit.

$$T_E^*(u) = \begin{cases} T_{\max} \operatorname{sgn}(u) & , |u| > T_{\max} \\ u & , |u| \leq T_{\max} \end{cases} \quad (3)$$

In this equation, u is the output of traditional PI controller, $\operatorname{sgn}(u)$ is the sign function.

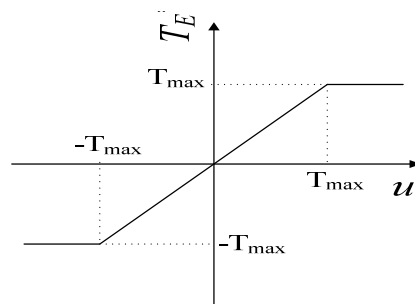


Figure 1. The Function Curve of $T_E^*(u)$

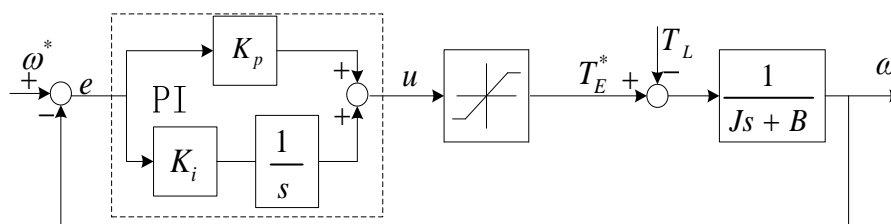


Figure 2. Traditional PI Controller Structure with a Saturation Limit

To inhibition the saturation phenomenon, this article introduced a new type Anti - Windup PI controller, figure 3 shows the control block diagram. According to the Figure 3, When $u = T_E^*$, switch S_1 will be closed, S_2 will be opened. The controller turns into the typical PI controller. When $u > T_E^*$, switch S_2 will be closed, S_1 will be opened. The output multiplied by a coefficient and then negative feedback to the input. So that the integral output can converges to zero rapidly.

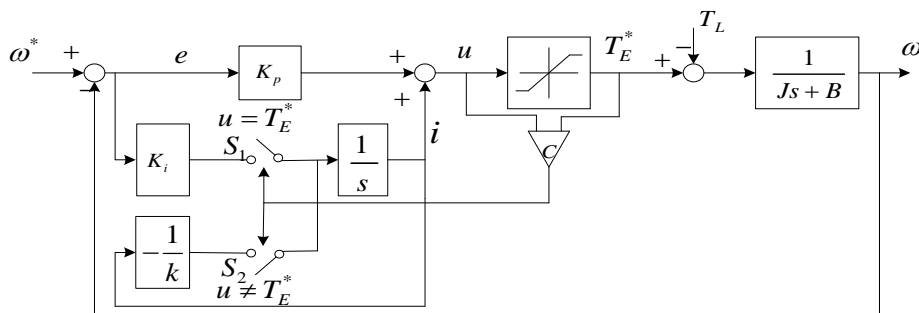


Figure 3. The New Anti-Windup PI Controller Structure

The i in the Figure 3 is integral state. Its expression is:

$$i = \begin{cases} \frac{K_i}{s} e, & u_s = u_n \\ -\frac{1}{k} i, & u_s \neq u_n \end{cases} \quad (4)$$

In Equation (4), K_i is integral constant. k is the integral feedback gain coefficients. And $k, K_i \ll k_m$.

3. Stability Analysis

If the system is stable, the system must meet two conditions. First the system in the linear region is stable. Second the system could convergence to the linear area from the saturated zone. If two conditions are satisfied at the same time, the system will be stable.

3.1. First Condition

In the linear, the new Anti-Windup PI controller is the same as traditional PI controller. At this time the error can be expressed as:

$$\dot{e} = \frac{\omega^*}{k_m} - \frac{(i - T_L)}{J} - \left(\frac{1}{k_m} + \frac{K_p}{J}\right)e \quad (5)$$

Lyapunov function is defined as follow:

$$L_1(e, i) = \frac{1}{2} \left(J e^2 + \frac{(i - i_0)^2}{K_i} \right) \quad (6)$$

In the Equation (6), i_0 is i 's stable value, so:

$$\dot{L}_1(e, i) = e \left[(B\omega^* + T_L) - i_0 \right] - \left(B + \frac{K_p}{J} \right) e^2 \quad (7)$$

$$i_0 = B\omega^* + T_L \quad (8)$$

In the linear, it always meets:

$$\begin{cases} \dot{V}_2(e, q) \leq 0 \\ i_0 \leq T_{\max} \end{cases} \quad (9)$$

To sum up, the controller's stable condition in the linear is:

$$\left| T_L \right| + B \left| \omega^* \right| \leq T_{\max} \quad (10)$$

3.2. Second Condition

In the saturated zone, we can get the expression of error from Equation (1).

$$\dot{e} = -\frac{e}{k_m} - \frac{(T_E^* - T_L)}{J} + \frac{\omega^*}{k_m} \quad (11)$$

From equation (4) we can get:

$$i = -\frac{i}{k} \quad (12)$$

Because of $k \ll k_m$, the dynamic speed error is far slower than the integral dynamic state. That is to say, the integral state i was immediately set to zero when the controller is in the saturated zone. So:

$$\begin{aligned} u &= K_p e + i \\ &= K_p e \end{aligned} \quad (13)$$

If $E_b = T_{max}/K_p$. From Equation (13), we can find that, when $|e| \leq E_b$ the controller is in the linear, when $|e| > E_b$ the controller is in the saturated zone.

Lyapunov function is defined as follow:

$$L_2(e) = \frac{e^2}{2} \quad (14)$$

After the derivation:

$$\begin{aligned} \dot{L}_2(e) &= e \times \dot{e} \\ &= -\frac{e^2}{k_m} + \left[\frac{\omega^*}{k_m} - \frac{(T_E^* - T_L)}{J} \right] e \end{aligned} \quad (15)$$

Take Equation (2) and Equation (13) into Equation (15)

$$\begin{aligned} \dot{L}_2(e) &= -\frac{e^2}{k_m} - \frac{T_{max}|e|}{J} + \left(\frac{T_L}{J} + \frac{\omega^*}{k_m} \right) e \\ &\leq -\frac{e^2}{k_m} + \left[\frac{\omega^*}{k_m} - \frac{(T_{max} - |T_L|)}{J} \right] |e| \end{aligned} \quad (16)$$

Because of $\dot{L}_1(e) \leq 0$, only need to meet:

$$|e| \leq k_m \left\{ -\frac{1}{J} (T_{max} - |T_L|) \right\} + |\omega^*| \quad (17)$$

So we can get the condition:

$$|T_L| + B|\omega^*| \leq T_{max} + \frac{B}{K_p} T_{max} \quad (18)$$

Compared Equation (10) and Equation (18), we can see that as long as the system meet Equation (10) must meet Equation (18). So Equation (10) is the stable condition.

To sum up we can get the stable condition as follow:

$$|T_L| + B|\omega^*| \leq T_{max} \quad (19)$$

4. Modeling and Simulation

Matlab/Simulink is used to carry out the modeling and simulation. Figure 4 is the structure chart of the DTC system with the new Anti-Windup PI controller. First of all, according to Figure 4 the model of induction motor DTC system with traditional PI controller was established. And then the model of the new Anti-Windup PI controller was established, shown in

the Figure 5. Finally the new Anti-windup PI controller replaced the traditional PI controller, so that we can get two different simulation diagrams of speed response.

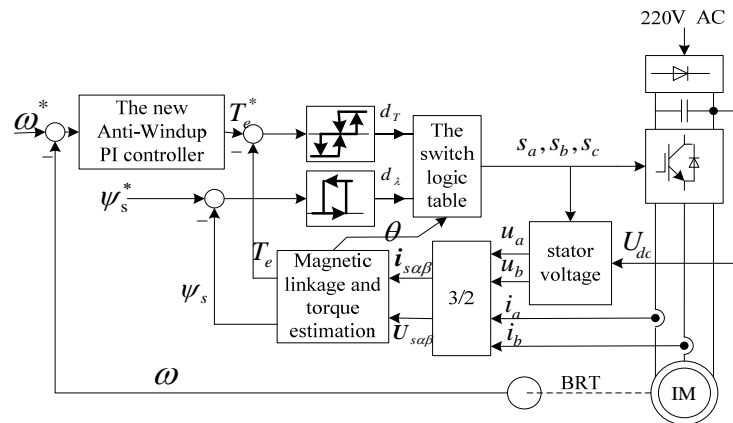


Figure 4. The Structure Chart of the System

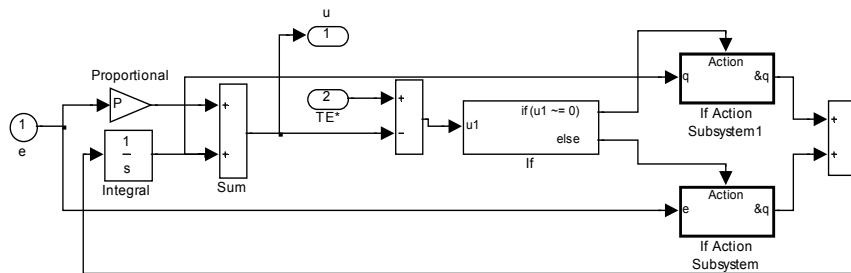


Figure 5. The New Anti-Windup PI Controller Simulation Diagram

5. Simulation and Experiment

5.1. The Simulation Results

Motor parameters are listed as follows: the stator resistance $R_s=2.5\Omega$, the rotor resistance $R_r=2.7\Omega$, the stator inductance $L_s=0.3325mH$, the rotor inductance $L_r=L_s=0.3325mH$, the mutual inductance $L_m=0.3194mH$, the logarithmic $P=2$, the moment of inertia $J=0.0086kg.m^2$. PI parameters is same in the two controllers, $K_p=1$, $K_i=10$. The integral feedback gain coefficients in the new Anti-Windup PI controller is $k=0.95$. The maximum output torque of the motor is $T_{max}=10N.m$, discrete sampling period is $50\mu s$. The stator flux linkage given value is $\psi^*=0.8Wb$.

Induction motor is starting with no load, but the load torque will become 4N.m at 1s. Speed is 0 at the beginning, then step to 400rad/s at 0.1s. Figure 6 is the results of simulation graphs. Figure 7 and Figure 8 are the partial enlarged figures.

From Figure 7 we can see that, traditional PI controller's overshoot amount of speed response reached 17.5% and adjustment time is 0.6s, but the new Anti-Windup PI controller is almost no overshoot amount of speed response and adjustment time is only 0.25s. From the simulation results can be seen, the new Anti-Windup PI controller's control performance has very obvious advantage.

From Figure 8 we can see that, when the load turns into 4N.m, the two curves are similar. Two types of controller's ability to resist load disturbance is almost the same.

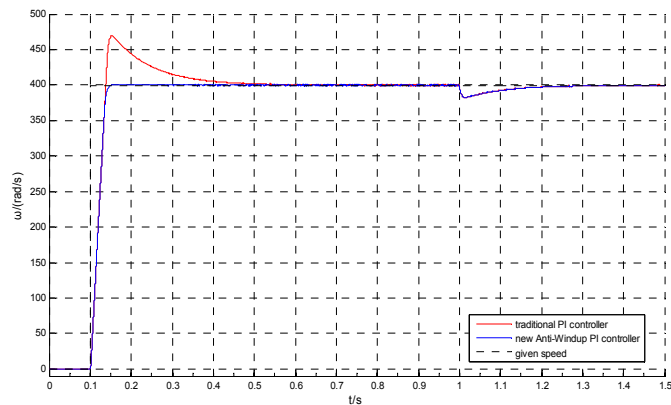


Figure 6. Simulation Result

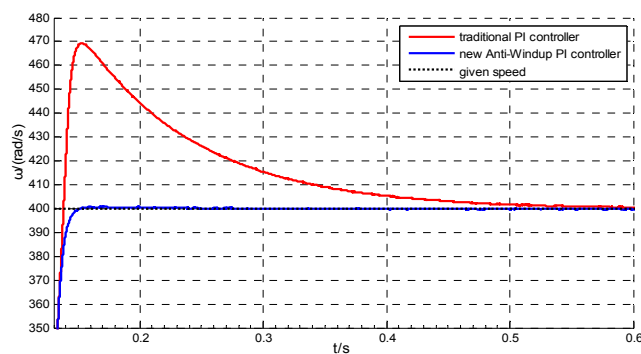


Figure 7. Partial Enlarged Graph of Speed Step Response

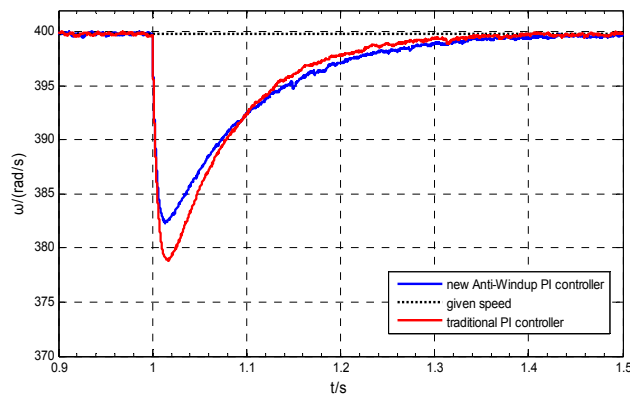


Figure 8. Partial Enlarged Graph of Joining the Load

5.2. Experimental Result

On the basis of theoretical analysis and digital simulation, this article has carried on the corresponding experimental research. Experiment system adopts the special motor control digital signal processor TMS320F2812 as the controller. Processor TMS320F2812 with RS - 232 serial communication ports will be collected experimental data transmitted to the PC.

The motor parameters are the same. The stator flux linkage amplitude to 0.8 Wb. Speed given value for 50 rad/s = 477.5 r/min. The load is about 1 N.m.

Figure 9 to 10 are the experimental results. The experimental results and simulation results are consistent. It validates the correctness of this method.

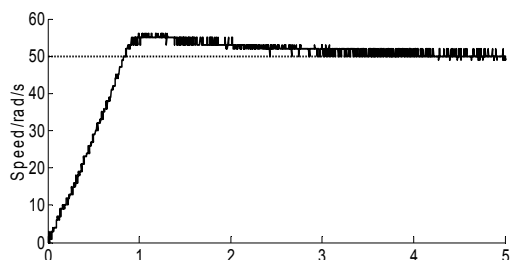


Figure 9. Experimental Results of Conventional PI Controller with Saturation Limits

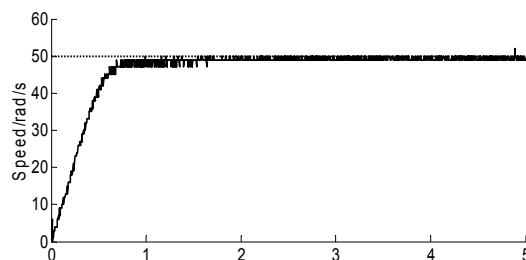


Figure 10. Experimental Results of New Anti-Windup PI Controller

6. Conclusion

The traditional PI controller has integral saturation problem, so this paper adopts a new type Anti-Windup PI controller. And the condition for the stability of the system is given. Simulation and experimental results show that, the new Anti-Windup PI controller can reduce or even eliminate overshoot amount of speed response, and shortens adjusting time. At the same time, the controller also has the advantages of simple structure and easy to project implementation.

References

- [1] Takahashi I, Naguchi T. A New Quick-response and High-efficiency Control Strategy of an Induction Motor. *IEEE Transaction on Induction Applications (S0093-9994)*. 1986; 22(5): 820-827.
- [2] M. Depenrock. Direct self-control of inverter-fed machine. *IEEE Transactions on Power Electronics*. 1988; 3(4): 420-429.
- [3] Wang Huan-gang, Xu Wen-li, Li Jian, et al. A new approach to direct torque control of induction machines. *Proceedings of the CSEE*. 2004; 24(1): 108-111.
- [4] S Tarbouriech, M Turner. Anti-windup design: an overview of some recent advances and open problems. *IET Control Theory and Applications*. 2009; 3(1): 1-19.
- [5] Sudhakar Ambarapu, M Vijaya Kumar. Neural Network Controllers in DTC of Synchronous Motor Drives. *TELKOMNIKA Indonesian Journal of Electrical Engineering*. 2013; 3(3): 311-320.
- [6] Yang Ming, Xu Dian-guo, Gui Xian-guo. Review of control system anti-windup design. *Electric Machines and Control*. 2006; 10(6): 622-626.
- [7] Zhou Hua-wei, Wen Xu-hui, Zhao Feng, et al. Predictive anti-windup strategy for PI-type speed controller. *Electric Machines and Control*. 2012; 16(3): 15-21.
- [8] Hwi-Beom Shin, Jong-Gyu Park. Anti-windup PID controller with integral state predictor for variable-speed motor drives. *IEEE Trans. Industrial Electronics*. 2012; 59(3): 1509-1516.
- [9] JK Seok, KT Kim, DC Lee. Automatic mode switching of P/PI speed control for industry servo drives using online spectrum analysis of torque command. *IEEE Trans. Industrial Electronics*. 2007; 54(5): 2642-2647.
- [10] Y Peng, D Vrancic, R Hanus. Anti-windup, bumpless, and conditioned transfer techniques for PID controllers. *IEEE Trans. Control Systems*. 1996; 16(4): 48-57.
- [11] Hwi-Beom Shin. New Antiwindup PI controller for variable-speed motor drives. *IEEE Trans. Industrial Electronics*. 1998; 45(3): 445-450.
- [12] Yu Yanjun, Chai Feng, Gao Hongwei, et al. Design of PMSM System Based on Anti-Windup Controller. *Transactions of China Electrotechnical Society*. 2009; 24(4): 66-70.
- [13] Jong-Woo Chi, Sang-Cheol Lee. Antiwindup strategy for PI-type speed controller. *IEEE Trans. Industrial Electronics*. 2009; 56(6): 2039-2046.
- [14] Miao JingLi, Huang Xiao Guang; Yuan Xiangmeng. Based on Anti-windup PI of brushless Dc motor control system design. *TELKOMNIKA Indonesian Journal of Electrical Engineering*. 2013; 2(12): 1278-1284.